Characteristics of Precipitating Convective Systems Accounting for the Summer Rainfall of Tropical and Subtropical South America

ULRIKE ROMATSCHKE AND ROBERT A. HOUZE JR.

University of Washington, Seattle, Washington

(Manuscript received 24 April 2012, in final form 15 August 2012)

ABSTRACT

Ten years of Tropical Rainfall Measuring Mission precipitation radar data are used to study the physical properties of the precipitating cloud systems that account for the summer rainfall of tropical and subtropical South America. Radar echoes in the continental subtropics tend to be of an intensely convective nature, especially at the eastern foothills of the Andes where diurnally forced deep convective cells of small horizontal scale form when moist low-level flow is driven toward the foothills in connection with a midlatitude disturbance. As the disturbance moves east over the La Plata basin, nocturnal convective systems of larger horizontal scale with wide stratiform regions occur in a zone of general convergence. Precipitation in the continental tropics is generally produced by convective systems with greater stratiform composition. At the northeastern foothills of the central Andes, radar echoes of nocturnal convective systems of medium to large horizontal scale occur where moist low-level flow is lifted over the foothills. Growth of systems to large size is inhibited by daytime divergence at the foothills. Over the Amazon basin, daytime systems are also smaller than nocturnal systems. Radar echoes of precipitation over the Brazilian Highlands are generally smaller in horizontal scale, more convective, and mostly occur during the afternoon over elevated terrain. In the oceanic South Atlantic convergence zone, radar echoes grow to extremely large sizes. They are highly stratiform in nature and occur during all times of the day except late evening when convergence is weakened as a response to continental heating.

1. Introduction

Convective cloud systems play an important role in the meteorology, climatology, and hydrology of South America. They not only produce the majority of the precipitation, especially in the tropical part of the continent, but are also associated with severe weather. Numerous studies show the influence of the synoptic regime on the development of convection and precipitation (Carvalho et al. 2002; Garreaud and Wallace 1998; Liebmann et al. 1999, 2004; Nieto Ferreira et al. 2003; Pereira and Rutledge 2006; Siqueira and Machado 2004; Siqueira et al. 2005; Lenters and Cook 1995, 1999; Petersen et al. 2002; Rickenbach et al. 2002; Zamboni et al. 2010). Other studies have focused on the mesoscale nature of the precipitating clouds, especially mesoscale convective systems (MCSs) (Houze 2004) and mesoscale convective complexes (MCCs) (Maddox 1980). The conditions leading to MCS and MCC development have been investigated for the bulk of the continent (Machado et al. 1998; Velasco and Fritsch 1987) as well as different subregions, such as southeastern South America (Anabor et al. 2008; Salio et al. 2007) and the Amazon basin (Halverson et al. 2002; Laurent et al. 2002). Garstang et al. (1994) described extremely large squall lines over the Amazon basin. Altinger de Schwarzkopf and Rosso (1982) and Silva Dias (2011) investigated the occurrence of tornadoes in southeastern South America and Brazil, respectively, and Mezher et al. (2012) and Matsudo and Salio (2011) investigated the occurrence of severe weather in Argentina. Romatschke and Houze (2010) analyzed the conditions that lead to extreme forms of convection throughout tropical and subtropical South America. The diurnal cycle of precipitation has been investigated over the Amazon basin (Angelis et al. 2004; Negri et al. 2000) and tropical and subtropical South America (De Angelis et al. 2004; Nogués-Paegle and Mo 1997).

These studies leave open the question of how the precipitation is related to the type of convective system producing the rain. It has remained unclear which types

Corresponding author address: Professor Robert Houze, Box 351640, Atmospheric Sciences, University of Washington, Seattle, WA 98195-1640.
E-mail: houze@uw.edu

DOI: 10.1175/JHM-D-12-060.1

of cloud systems dominate the precipitation production in the different regions and over the whole continent. The goal of our study is therefore to link the types of convective phenomena with the type and amount of precipitation in the major precipitation regions of tropical and subtropical South America. Data from the Tropical Rainfall Measuring Mission (TRMM) precipitation radar (PR) are ideal for studying the connection between convection and precipitation since they provide comprehensive coverage of the region, determine the rainfall amounts, and describe the three-dimensional (3D) reflectivity structures of precipitating convective systems from which the nature of the convective cloud systems can be determined. From the TRMM PR dataset we address the following specific questions for tropical and subtropical South America.

- How much of the total surface precipitation is accounted for by different types of convective systems?
- What is the geographical distribution of the types of convective phenomena accounting for most of the rainfall?
- What are the physical characteristics of the convective cloud systems producing most of the rainfall?
- What meteorological and topographical factors determine the occurrence of the different types of convection?

By answering these questions we will ascertain the nature of the convection that is most and least important for producing rain over tropical and subtropical South America as a whole and in different subregions. We further aim to improve knowledge of the fundamental mechanisms that determine the development of these different types of cloud systems and need to be implemented in weather and climate prediction models.

2. Data

As noted above, the main data source for this study is the TRMM PR (Kummerow et al. 1998, 2000). The specific products used are

- 2A23 rain characteristics (Awaka et al. 1997), which classifies each vertical reflectivity column as "convective," "stratiform," or "other";
- 2A25 rainfall rate and profile (Iguchi et al. 2000), which provides the 3D radar reflectivity data;
- 3A25 spaceborne radar rainfall (Meneghini et al. 2001), which provides monthly counts of the total number of pixels on a 0.5° × 0.5° grid that are used to normalize the reflectivity data from the strongly latitude-dependent orbit of the TRMM satellite.

A detailed description of the data processing and analysis methods is given in Romatschke and Houze

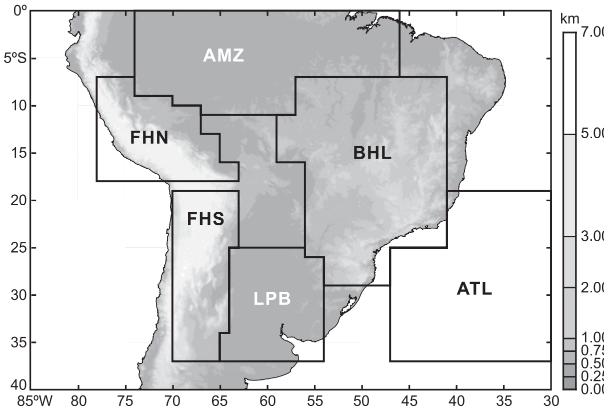

FIG. 1. Topography of the region of interest and subregions: La Plata basin (LPB), western South Atlantic (ATL), Brazilian Highlands (BHL), Amazon basin (AMZ), northeastern and southeastern foothills of the Central Andes (FHN and FHS, respectively). Higher topography is in lighter shading.

(2011a). In brief, the irregularly spaced 3D reflectivity and rain characteristics data are remapped onto a latitude–longitude height grid with 0.05° horizontal and 0.25-km vertical resolution using the interpolation method described in Houze et al. (2007) on each reflectivity pixel. For the rain characteristics data a "nearest neighbor" approach was used. Within the remapped reflectivity data we search for contiguous echo objects. These objects are fundamental components of precipitating convective cloud systems. The surface rain rates for each echo object are calculated from the reflectivity values that are closest to the surface. Echo objects that cover only one pixel in the horizontal are neglected. The precipitation from all echo objects combined and from certain subsets of them are added and normalized with the overpass frequency of the satellite in the respective regions. Our analysis is based on the austral summer months (December–February) of 10 years of data from December 1998 to February 2008.

Thirty years of data of the austral summer months (December 1979–February 2010) from the National Centers for Environmental Prediction (NCEP) Climate Forecast System Reanalysis (CFSR) have been used to show the climatology of the 10-m winds and divergence calculated thereof. The data used are available every six hours as a 6-h forecast with a horizontal resolution of 0.5°.

The region of interest extends from 0° to 37°S, 30° to 85°W (Fig. 1) and includes all the major precipitation regions of tropical and subtropical South America (see Romatschke and Houze 2010, their Fig. 2a). Based on the precipitation characteristics and the geographical distribution of the different types of precipitation systems examined in this paper, we will refer to six subregions:

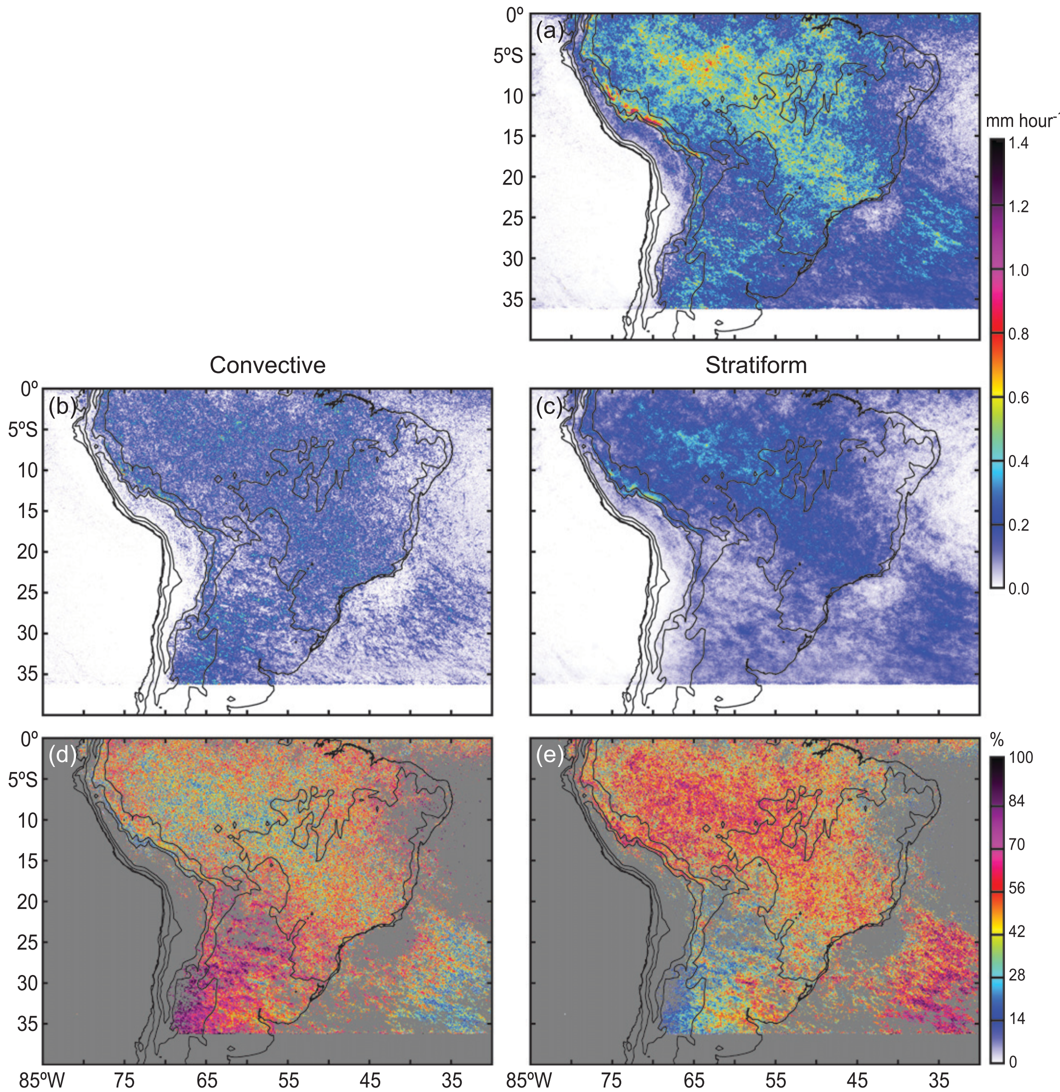

FIG. 2. Summer precipitation means of (a) total rain, (b) convective rain, (c) stratiform rain, (d) convective percentage, and (e) stratiform percentage. Pixels where the total precipitation is <0.15 mm h^{-1} are deleted. Topographic contours of 0.3 km, 1.5 km, and 3 km are shown in black.

Amazonia (AMZ), the Brazilian Highlands (BHL), the southwest Atlantic (ATL), the northeastern and southeastern foothills of the Central Andes (FHN and FHS, respectively), and the La Plata basin (LPB).

3. Geographical distribution of precipitation from convective systems

a. *Overall, convective, and stratiform precipitation patterns*

Figure 2a shows the overall summer precipitation in tropical and subtropical South America. The most prominent precipitation region stretches from the AMZ region (Fig. 1) to the southeast over the BHL region. The absolutely highest amounts, however, are closely tied to terrain in a separate, much smaller region in the FHN region. Secondary precipitation regions extend from the FHS over the LPB regions and over the ATL region.

Averaged over the whole region of study, the precipitation is classified as 45% convective and 46% stratiform. Interestingly these numbers are almost exactly the same as have been observed in the South Asian monsoon (Romatschke and Houze 2011a) and therefore may be representative for precipitation in the wet phase of a monsoon-like regime.

Over Amazonia, and to a lesser extent over the Brazilian Plateau, the precipitation has a large percentage of stratiform rain (Figs. 2c,e). This pattern shows that the major summertime precipitation region of South America is dominated by convective systems with large stratiform components.

In the regions with less precipitation, in the foothills of and just east of the southern Andes (FHS), the precipitating cloud systems produce very little stratiform rain; the radar echoes are mostly of a convective nature (Figs. 2b,d), in sharp contrast to the large stratiform components seen in the AMZ and BHL region (cf. Figs. 2c,e). It has been noted previously by Zipser et al. (2006), Houze et al. (2007), Romatschke et al. (2010), and Romatschke and Houze (2010, 2011a,b) that arid regions near both the Himalayas and Andes tend to have intense precipitation of a highly convective nature.

b. Echo objects by size and region

To investigate the characteristics of different types of precipitating cloud elements, we identify contiguous echo objects and divide them into four categories of areal coverage as

- Smallest: <950 km^2
- Small: 950–14 500 km^2
- Medium: 14 500–47 000 km^2
- Large: >47 000 km^2.

Following Romatschke and Houze (2011a), this subdivision was carried out in such a way that the radar echo objects in each of the three larger categories contribute 30% to the total precipitation and are therefore equally important from a hydrological point of view. The smallest echoes contribute the remaining 10% to the total precipitation and, although they are extremely large in number (Fig. 3a), they are not further investigated in this study because of their small precipitation production.

Figure 3a shows the total number of radar echo objects in each category on a log scale. The number decreases exponentially with increasing echo size, indicating [as was found in South Asia (Romatschke and Houze 2011a,b)] that horizontal size is the most important characteristic of a precipitating cloud system in determining its precipitation production. Although the total amounts of convective and stratiform precipitation are almost equal (section 3a), the amount of stratiform precipitation increases with increasing radar echo size, while the proportion of convective precipitation decreases (Fig. 3b); that is, smaller echoes tend to be more convective than larger ones, which we also found to be the case in South Asia.

Figure 4 shows the geographical distribution of small, medium, and large echo objects and their contribution to the overall precipitation. Small radar echo objects occur most frequently near the equator, along the edge

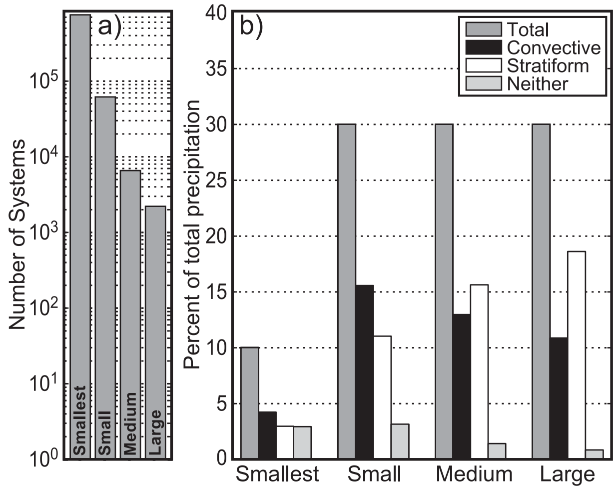

FIG. 3. (a) Total number of echo objects in the four size categories defined in the text. (b) Percentage that each type of system contributes to the total precipitation.

of the Andes (FHN and FHS), and over the Brazilian Highlands (BHL) (Figs. 4a,b). The high concentrations of rain and frequency of small echoes along the edges of both regions of higher terrain link the small systems to terrain gradients. In general, small systems tend to occur in regions with little rain (cf. Figs. 2a and 4b). Medium and large echo objects occur and produce precipitation throughout all major precipitation regions (Figs. 4c–f). Cloud systems with large contiguous echoes are the dominant precipitation producers over the plains of Argentina (LPB) as well as over the ocean (ATL), whereas precipitation over the Amazon basin (AMZ) comes from both large and medium systems.

4. Physical properties of precipitating convective systems

a. General characteristics

To investigate the characteristics that make a convective cloud system produce a lot of rain, we follow the procedure of Romatschke and Houze (2011a) by first sorting the contiguous echo objects in each size category and geographical subregion according to their volumetric rain rate [local rain rate (kg m^{-2} s^{-1}) × area (m^2)]. Then we further subdivide the systems into two groups about their volumetric rain rate median. The "strong" echoes are those with volumetric rain rates exceeding the median value, and the "weak" ones with rates less than the median. A few strong echoes constitute the same amount of rain as many weak ones. Table 1 shows the number of total, strong, and weak echo objects in each size category and region and the percentage of precipitation that comes from the echoes in a specific size

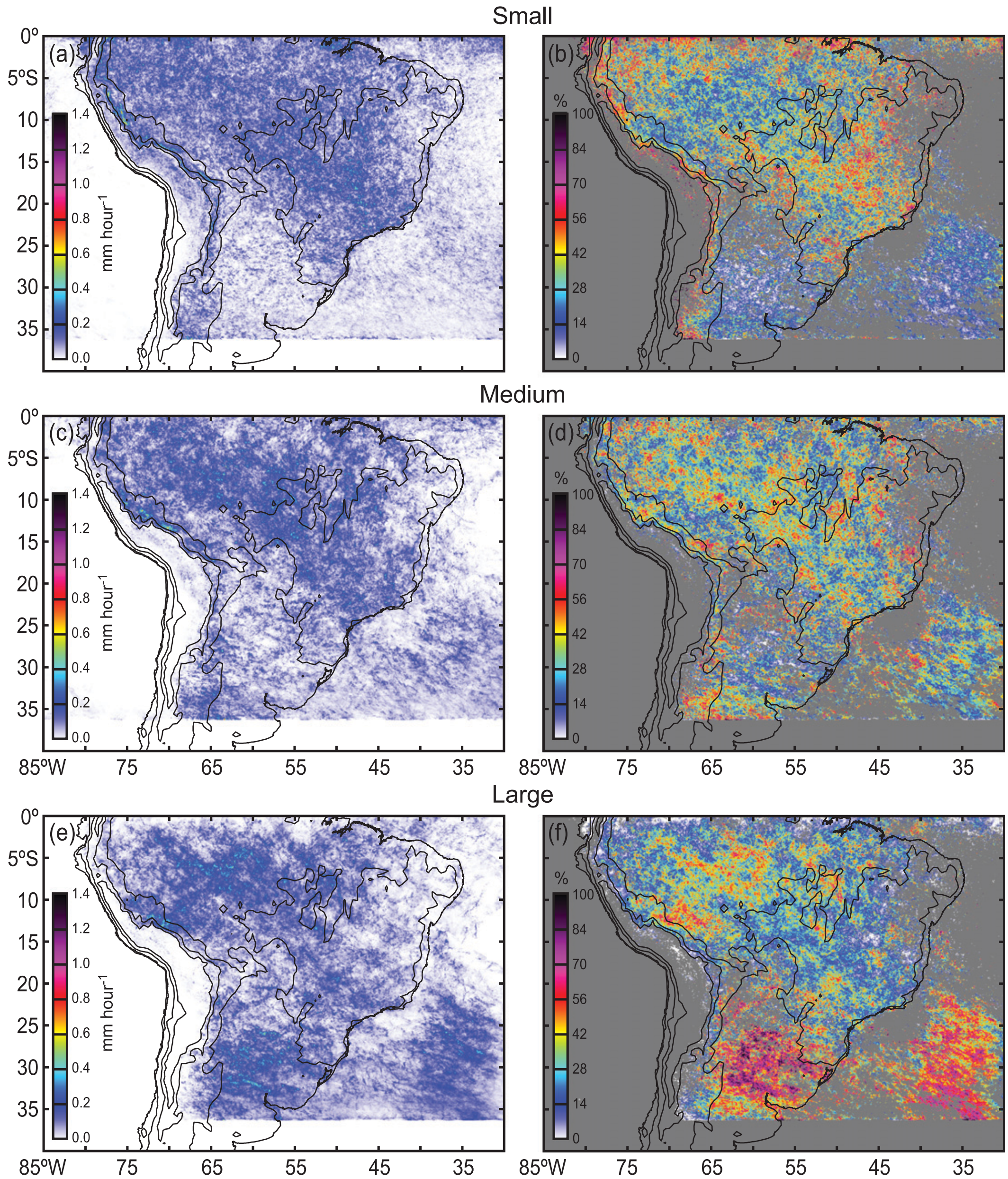

FIG. 4. Precipitation patterns from small, medium, and large echoes: (left) total rain and (right) percentage. Orographic contours as in Fig. 2.

category in a specific region. Only categories where the contribution to the precipitation is over 20% are shown and further investigated.

Tables 2, 3, and 4 show the physical properties of small, medium, and large echo objects, respectively, and the differences between the total, weak, and strong ones. The specific characteristics shown are

- mean total area covered by echo objects in each echo category—as a measure of the horizontal extent of the systems;
- mean altitude of the highest convective radar pixel with a reflectivity value equal to or greater than 40 dBZ in the contiguous echo objects—as a measure of the depth of embedded convective cells;
- horizontal area of the convective pixels with reflectivities over 40 dBZ divided by the total area—as a measure of horizontal extent of intensive convective regions;
- convective and stratiform rain fractions—as metrics of the contribution of convective and stratiform rain to the total precipitation of the echoes.

TABLE 1. Echo size statistics. The percentage of rain in each region accounted for by small, medium, and large radar echoes. Also indicated are the total number of echo objects in each category and the number of those objects categorized as weak or strong.

	FHS	LPB	FHN	AMZ	BHL	ATL
	Small					
Rain (%)	39.4		34.2	31.4	33.2	
Total	3461		4757	13 184	15 363	
Strong	496		681	1926	2290	
Weak	2965		4076	11 258	13 073	
	Medium					
Rain (%)	33.1	26.0	28.6	32.0	32.3	28.1
Total	335	482	382	1409	1715	1058
Strong	95	124	103	415	512	254
Weak	240	358	279	995	1203	804
	Large					
Rain (%)		56.2	25.7	27.7	25.8	45.7
Total		276	89	393	455	588
Strong		69	26	120	140	150
Weak		207	63	273	315	438

TABLE 2. Small-echo properties. Mean total area (km^2) covered by weak, strong, and all echo objects in the small category (smallest of the 30% size categories). Also indicated are the mean convective 40-dBZ echo area fraction (%), maximum 40-dBZ echo height (km), convective rain fraction, and stratiform rain fraction (%) of echoes in the small size category.

	FHS	FHN	AMZ	BHL
	Total area			
All	3327	3166	3233	3235
Strong	7473	7860	8044	7898
Weak	2634	2381	2410	2418
	Convective 40-dBZ area/total area			
All	6	2	4	5
Strong	16	6	8	11
Weak	5	2	3	4
	Convective 40-dBZ height			
All	3.7	1.9	2.2	3.0
Strong	8.8	4.9	5.0	6.2
Weak	2.9	1.4	1.8	2.4
	Convective rain fraction			
All	44	28	37	40
Strong	79	47	56	61
Weak	38	24	34	37
	Stratiform rain fraction			
All	39	52	47	45
Strong	16	43	37	32
Weak	43	53	48	47

In all echo object categories, strong echoes are larger than weak ones, confirming that size is important for precipitation production (section 3b). However, the convective nature of the echo also plays an important role. In all categories, the convective characteristics are more pronounced and the stratiform rain fractions are less for the strong echoes than for the weak. The difference between the strong and weak echoes is greatest for small echoes and decreases with echo size. This reverse behavior between convective characteristics and size indicates that the convective nature plays a more important role for precipitation production when the cloud systems do not grow to large horizontal scale or the convection is in an early, and hence smaller, stage of life cycle, whereas at later stages horizontal size dominates. However, even for the large convective systems, embedded convective cells help to increase precipitation production.

In general, the depth of the convective echo objects exceeding 40 dBZ increases with echo size; however, as just pointed out, the increased depth of the convective cells in the large echoes plays a secondary role in the precipitation production compared to size alone. In contrast, large echo objects have larger stratiform rain fractions, which is not surprising given the fact that they most likely represent convective systems in a mature or late stage of their life cycle when early convective cells have aged to form large stratiform regions (Houze 2004; Romatschke and Houze 2010).

b. Characteristics of echo objects in different regions

We have seen that in the two regions located in the continental subtropics (FHS and LPB), precipitation comes from convective systems that have a more actively convective character than do systems in any other region (section 3a, Fig. 2). Especially noteworthy, the radar echoes in the FHS region are extremely deep with the 40-dBZ echoes of strong medium echo objects reaching up to 10 km in height on average (Table 3). The convective rain fraction in the FHS is significantly larger than in any other region, even larger than in the LPB region (e.g., 57% versus 49%, respectively, for medium systems; see Table 3). The very convective nature of the systems in the continental subtropics agrees with the results of Zipser et al. (2006) and Romatschke and Houze (2010), who found a maximum of extremely deep convective cores in this region. Despite the similarities of the characteristics of precipitating systems in the FHS and LPB region the amount of precipitation coming from different system categories are very different:

TABLE 3. As in Table 2 but for the medium category (middle group of the 30% size categories).

	FHS	LPB	FHN	AMZ	BHL	ATL
	Total area					
All	25 115	28 207	24 372	26 267	25 543	27 339
Strong	31 337	35 308	33 508	34 866	33 363	35 802
Weak	22 652	25 748	21 000	22 677	22 215	24 665
	Convective 40-dBZ area/total area					
All	8	9	3	4	5	4
Strong	15		6	6	8	8
Weak	6	6	2	3	3	2
	Convective 40-dBZ height					
All	7.6	6.3	4.9	4.6	5.3	3.7
Strong	10.1	9.4	6.0	5.7	6.8	5.4
Weak	6.6	5.2	4.5	4.2	4.6	3.1
	Convective rain fraction					
All	57	49	33	35	37	29
Strong	78	73	43	42	47	45
Weak	49	41	30	32	33	24
	Stratiform rain fraction					
All	38		59	60	57	66
Strong	20	25	52	54	49	53
Weak	45	53	61	62	61	69

TABLE 4. As in Table 2 but for the large category (largest of the 30% size categories).

	LPB	FHN	AMZ	BHL	ATL
	Total area				
All	82 735	75 589	73 307	74 063	81 034
Strong	121 254	105 287	96 162	99 302	107 809
Weak	69 895	63 333	63 261	62 846	71 865
	Convective 40-dBZ area/total area				
All	9	4	4	4	3
Strong	15	6	6	6	6
Weak	8	3	3	3	2
	Convective 40-dBZ height				
All	8.2	5.7	5.4	6.0	4.3
Strong	10.4	6.1	5.9	7.1	5.5
Weak	7.4	5.6	5.2	5.3	3.9
	Convective rain fraction				
All	47	29	29	30	23
Strong	58	33	34	38	33
Weak	43	27	27	26	19
	Stratiform rain fraction				
All	51	67	67	67	75
Strong	41	65	64	59	65
Weak	55	68	69	70	78

in the FHS region precipitation comes mostly from small and medium systems (39% and 33%, respectively, Table 1), whereas in the LPB region most of the precipitation comes from large systems (56%, Table 1). As has been shown previously for different types of convective systems (Altinger de Schwarzkopf and Rosso 1982; Anabor et al. 2008; Garreaud and Wallace 1998; Nicolini and Saulo 2006; Romatschke and Houze 2010), the systems in our small and medium size categories in the FHS region systematically move eastward over the LPB region, in association with a midlatitude disturbance, where they grow into large systems (plots not shown).

The physical properties of the medium and large systems that produce the precipitation in the continental tropics, that is, in the FHN and AMZ regions, are very similar in the two regions. Small systems are slightly more convective in the AMZ than in the FHN region: for example, the convective rain fractions are 37% versus 28%, respectively (Table 2). For all size categories the stratiform rain fraction is larger than the convective rain fraction, in agreement with findings of systems featuring extremely large stratiform precipitation regions (Romatschke and Houze 2010). Precipitation in these regions comes from all three categories of system size with almost equal amounts, and only slightly decreases with system size (Table 1).

Echo objects associated with precipitation in the two regions located in the South Atlantic convergence zone (SACZ), that is, the BHL and ATL regions, have different characteristics in each region, which supports our choice to study these regions separately. In the BHL region the echo objects have a generally more convective nature than in the ATL region. The embedded convective cells penetrate higher into the atmosphere and are even deeper than the convective cells in the FHN and AMZ regions, consistent with the occurrence of extremely deep convective cores in this region (Romatschke and Houze 2010). The convective rain fraction in the BHL is also larger than in the ATL region, which in contrast has the largest stratiform rain fraction of all regions. The large stratiform rain fraction of the systems in the ATL region is likely associated with system containing extremely large stratiform echo areas in this region (Romatschke and Houze 2010). In the BHL region, precipitation is mostly accounted for by small and medium systems with large systems contributing less but also significantly, whereas in the ATL region precipitation comes predominantly from large and less from medium systems (Table 1). The systems that produce the precipitation in the ATL region are associated with low pressure over that region (plots not shown) as has been pointed out for echo objects containing extremely large stratiform regions by Romatschke and Houze (2010).

5. Diurnal and regional variability of precipitating cloud systems

Figure 5 shows the pronounced classic diurnal cycle of 10-m winds and divergence associated with the Andes as shown by the NCEP CFSR fields described in section 2. During the afternoon increased solar heating over the Andes leads to strong convergence over the mountains, upslope flow at the slopes, and divergence at the foothills (Fig. 5c). During the night and morning the pattern is reversed: cooling over the mountains leads to downslope flow, divergence over the mountains, and convergence over the adjacent plains (Figs. 5a,b). In the following subsections, we will see that this cycle has a profound effect on the development of precipitating convective systems.

a. Continental subtropics

In the FHS region precipitation comes primarily from small radar echoes (section 4b), which likely represent young convection and occur preferentially in the afternoon (Figs. 6a,b). Precipitation from convective systems of small horizontal dimension first appears over the slopes of the Andes (Fig. 7c) where solar heating induces lifting over the terrain and triggering of convective cells over the crests (Fig. 5c). The diurnal lifting over the terrain is key to releasing the convection since the moist low-level flow from the Atlantic and/or Amazon region tends to be capped by dry westerlies that subside on the lee side of the mountains (Rasmussen and Houze 2011). In the evening, precipitation associated with these systems occurs over the lowlands (Fig. 7d). The later initiation of small convective echoes over the plain is probably due to the convection being triggered by solar heating without the aid of lifting over the steep terrain. In the late night and morning hours, small echoes either dissipate or grow to larger sizes and are then represented in the medium size category (Figs. 8a,b). Small echoes in the LPB region also occur mostly in the afternoon (Fig. 6b); however, they only contribute 15% to the total precipitation there whereas in the FHS they contribute 39% (section 4b, Table 1).

Medium-sized echo objects, which are associated with a significant amount of precipitation in the FHS region, peak in occurrence around midnight after the peak in small systems (Fig. 6c), indicating that the small systems have grown upscale. The medium echo objects are mostly located over the plains near the foothills of the FHS region (Fig. 8a), in the region of convergence at the base of the mountains (Fig. 5a), where the nocturnal downslope flow converges with the diurnally modulated South American low-level jet (SALLJ) (Marengo et al. 2004; Romatschke and Houze 2010; Rasmussen and Houze 2011). Over the LPB region the diurnal cycle of medium convective systems is weak (Fig. 6d) and their locations are scattered over the whole region.

Large echo objects are rare in the FHS region and therefore contribute little to the precipitation (section 4b, Table 1), but the few large echoes that do occur peak even later than the medium systems (Fig. 6e), indicating a further upscale development. In the LPB region, large echo objects contribute the majority of the precipitation (section 4b, Table 1), which agrees with the results of Durkee et al. (2009), who found that a significant portion of precipitation in this region is contributed by large MCCs, although the MCC contribution that they noted is on the north edge of the LPB region. Large echo objects in the LPB region peak in the morning hours (Fig. 6f), which agrees with the results of Nesbitt and Zipser (2003), who found a peak in MCSs in the morning hours in subtropical South America. The nocturnal and morning systems over the LPB are a manifestation of the overall peak of nocturnal precipitation in this region (Kikuchi and Wang 2008). Further, it is well known that mesoscale convective systems tend to develop initially from convective cells triggered in the afternoon in the FHS region (Fig. 6a). Collections of cells merge while generally moving eastward, often in connection with a trough in the midlevel westerlies and a front forcing at low levels. They grow larger in scale and eventually develop into mesoscale convective systems with large stratiform rain areas (Nicolini and Saulo 2006; Saulo et al. 2007; Matsudo and Salio 2011; Rasmussen and Houze 2011). The mesoscale systems that develop from diurnally initiated convection are maintained for their subsequent lifetimes by continued triggering of new convection by convergence along a front and/or by the cold pool spreading from the mesoscale system. The statistics in Fig. 6 are consistent with this knowledge of storm behavior—from which we expect that, once the mesoscale storms develop from smaller scale, the convection triggered diurnally over the lower hilly terrain of the FHS (Fig. 6a) moves with an eastward component, manifesting as large echo objects in early midmorning (Fig. 6f). The nocturnal-to-early-morning maximum is aided by the input of moisture by the diurnally modulated SALLJ. Consistent with this type of storm movement and evolution, the time sequence

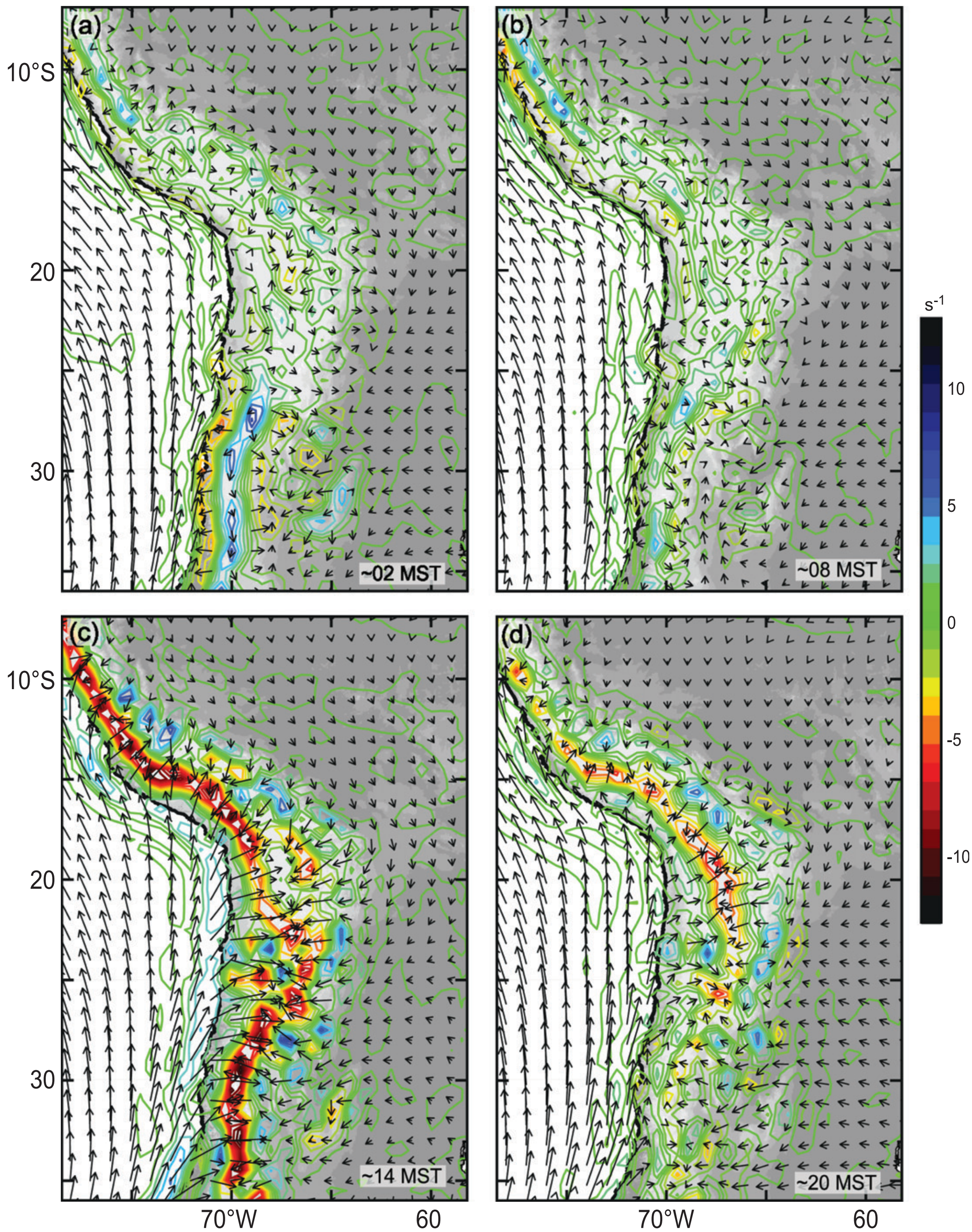

FIG. 5. NCEP CFSR 10-m winds (m s^{-1}) and divergence (s^{-1}) climatology at (a) 0600 UTC (~0200 MST), (b) 1200 UTC (~0800 MST), (c) 1800 UTC (~1400 MST), and (d) 0000 UTC (~2000 MST), MST ≡ mean solar (local) time. For better readability the wind vectors are shown at 1° resolution.

maps of the precipitation from large radar echoes (Figs. 9a–c) show that the preferred location of the large echoes shifts from southwest to northeast over the day with maximum coverage in the midnight-to-noon time frame. Figure 6e shows the occurrence of strong large echo objects tending to peak earlier in the day than the weak large echo objects. The later occurrence of weak echoes would be consistent with them representing a very late stage of mesoscale system development when convective cores, which are important for precipitation production (section 4a), are in less abundance.

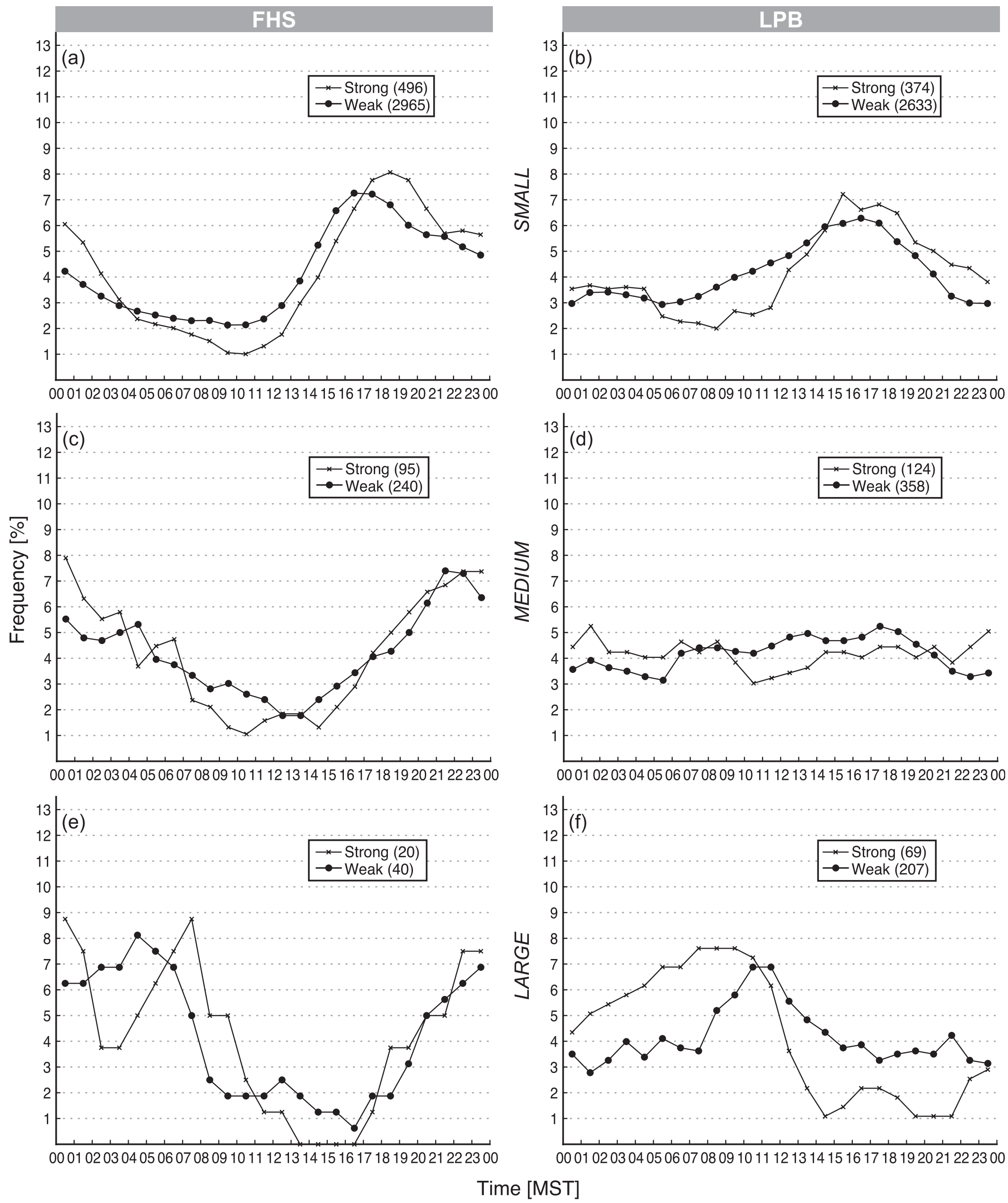

FIG. 6. Diurnal cycles of strong and weak small, medium, and large echoes in the FHS and LPB regions.

Since the frequency of the TRMM snapshots is too low to investigate the evolution of single systems, the system development from small to medium and large can only be assumed from a statistical approach like the one carried out here. However, the diurnal cycles and locations of the echo object-size categories just described suggest consistency with the scenario, suggested by previous papers (Anabor et al. 2008; Romatschke and Houze 2010; Rasmussen and Houze 2011), according to which systems of small horizontal dimension are triggered in the afternoon—first at the slopes of the Andes, breaking through the cap with the help of upslope flow, and later over the plains. During the night they grow to medium size in the FHS region as the downslope flow converges with the SALLJ, which brings moisture from the Amazon basin. In the morning they grow to large sizes. Embedded in midlevel westerly to southwesterly flow, they move, sometimes together with baroclinic disturbances, to the northeast over the LPB region where they weaken and dissipate. Anabor et al. (2009) suggested that not

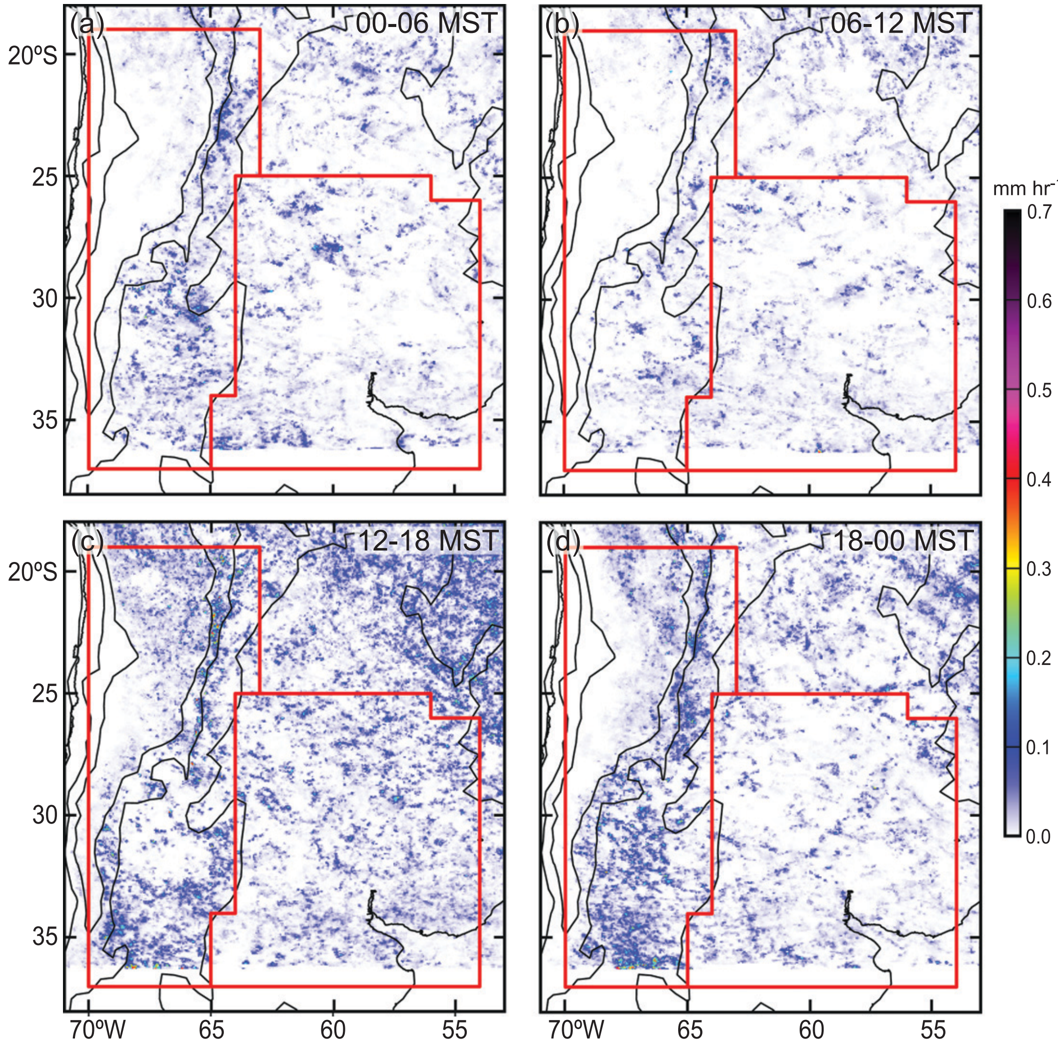

FIG. 7. Precipitation from small systems occurring (a) between 0000 and 0600 MST, (b) between 0600 and 1200 MST, (c) between 1200 and 1800 MST, and (d) between 1800 and 0000 MST in the continental subtropics. Orographic contours as in Fig. 2; the outlined regions are defined in Fig. 1.

only synoptic and topographic forcing but also internal gravity waves and triggering of convection by cold pools from earlier convection contribute to the development and propagation of the convection in southeastern South America.

b. Continental tropics

As in the continental subtropics, small convective systems peak in the afternoon in the tropical FHN and AMZ regions (Figs. 10a,b), undoubtedly as a result of solar heating. At that time precipitation from these systems is scattered over the whole region with maxima on the slopes of the Andes in the FHN region and in the northwest corner of the AMZ region in Fig. 11c, which lies near the mouths of the Amazon River and the Rio Tocantins. During the night regional maxima appear at the lower Andes slopes and foothills, which are likely caused by local small-scale effects (Figs. 11d,a).

Medium convective radar echoes contribute a little less precipitation than small echoes in the continental tropics (Figs. 4a–d, Table 1, section 4b). Strong and weak medium echo objects peak in occurrence at different times of the day in the FHN region (Fig. 10a). The same is true for the relatively small number of strong and weak large echo objects seen in this region (Fig. 10c). Weak medium and weak large echoes in the FHN region are most frequent in the afternoon, probably as a result of solar heating, and their precipitation is scattered evenly over the foothills and adjacent plains (Figs. 12c and 13c). During the late night and morning precipitation from strong, medium, and large convective systems, which have a broad peak in their

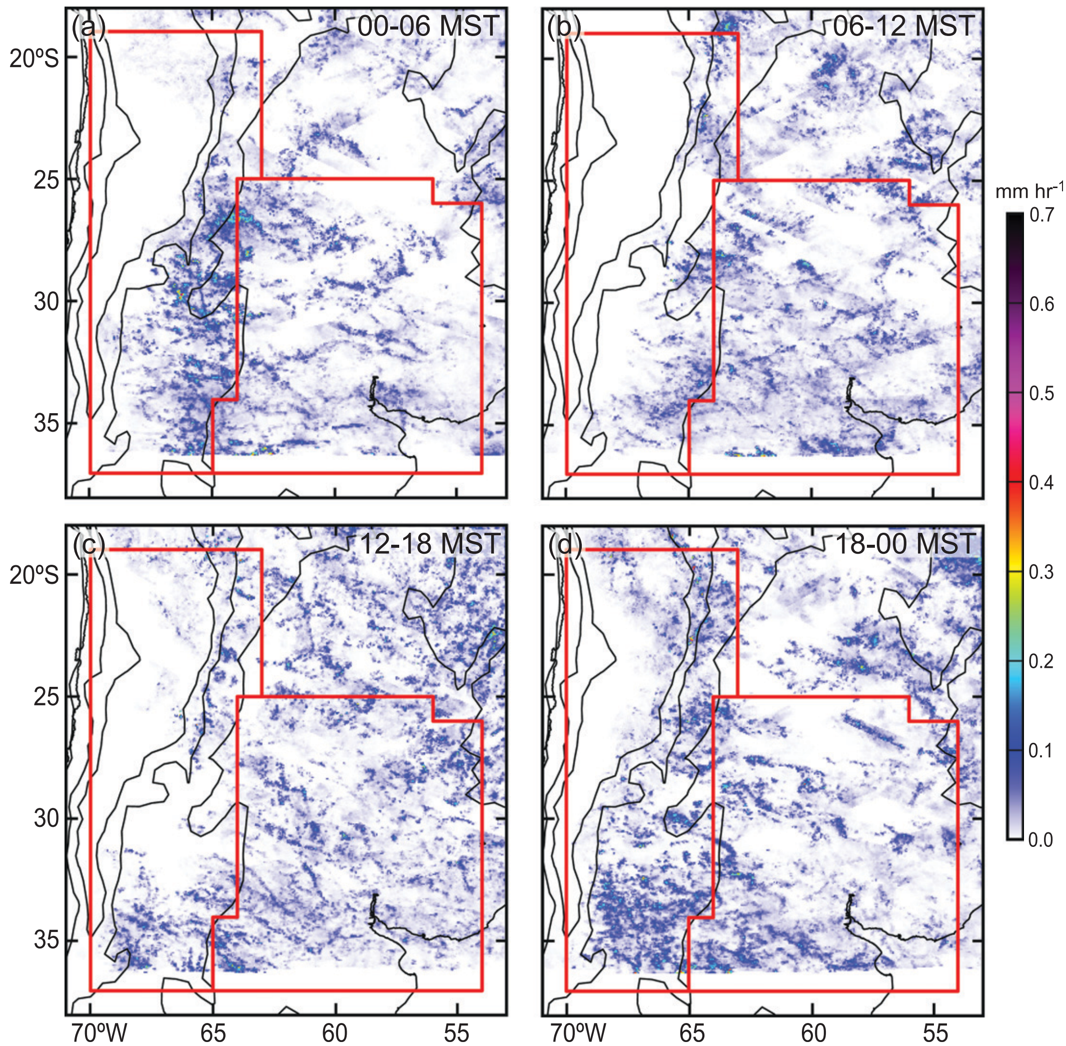

FIG. 8. As in Fig. 7 but for medium echoes.

diurnal cycle during these times (Figs. 10a,c), occurs at the Andes foothills closely following the terrain (Figs. 12a,b and 13a,b). These strongly precipitating systems are likely associated with a nocturnal precipitation and cloud cover maximum at the Andes foothills (Garreaud and Wallace 1997; Kikuchi and Wang 2008), which is unusual for continental regions where, in general, diurnal precipitation maxima prevail (Kikuchi and Wang 2008). The mechanisms that lead to the occurrence of the nocturnal precipitation are likely similar to the ones described by Romatschke and Houze (2010) for echo objects featuring extreme characteristics: moist northerly winds from the Amazon basin are lifted over the slopes and likely converge with nocturnal downslope winds, probably a result of the divergence over the mountains, which leads to convection at the foothills of the Andes. These mechanisms, also noted by Giovannettone and Barros (2009), lead to increased precipitation during the night since during the afternoon and evening the strong convergence over the mountains leads to divergence over the foothills (Figs. 5c,d), thus hindering the development of strongly precipitating convective systems. Similar mechanisms likely produce a nocturnal maximum of convective systems and precipitation at the foothills of the Himalayas where nocturnal downslope flow converges with moist flow from the Bay of Bengal (Romatschke and Houze 2011a).

The diurnal cycles for medium and large echo objects are less pronounced than the diurnal variation of the echoes with small horizontal dimensions; however, they are noticeable and are similar to each other (Figs. 10d,f). Weak echoes peak in the afternoon in association with solar heating whereas strong echoes show a two-peak structure with one peak in the afternoon and another

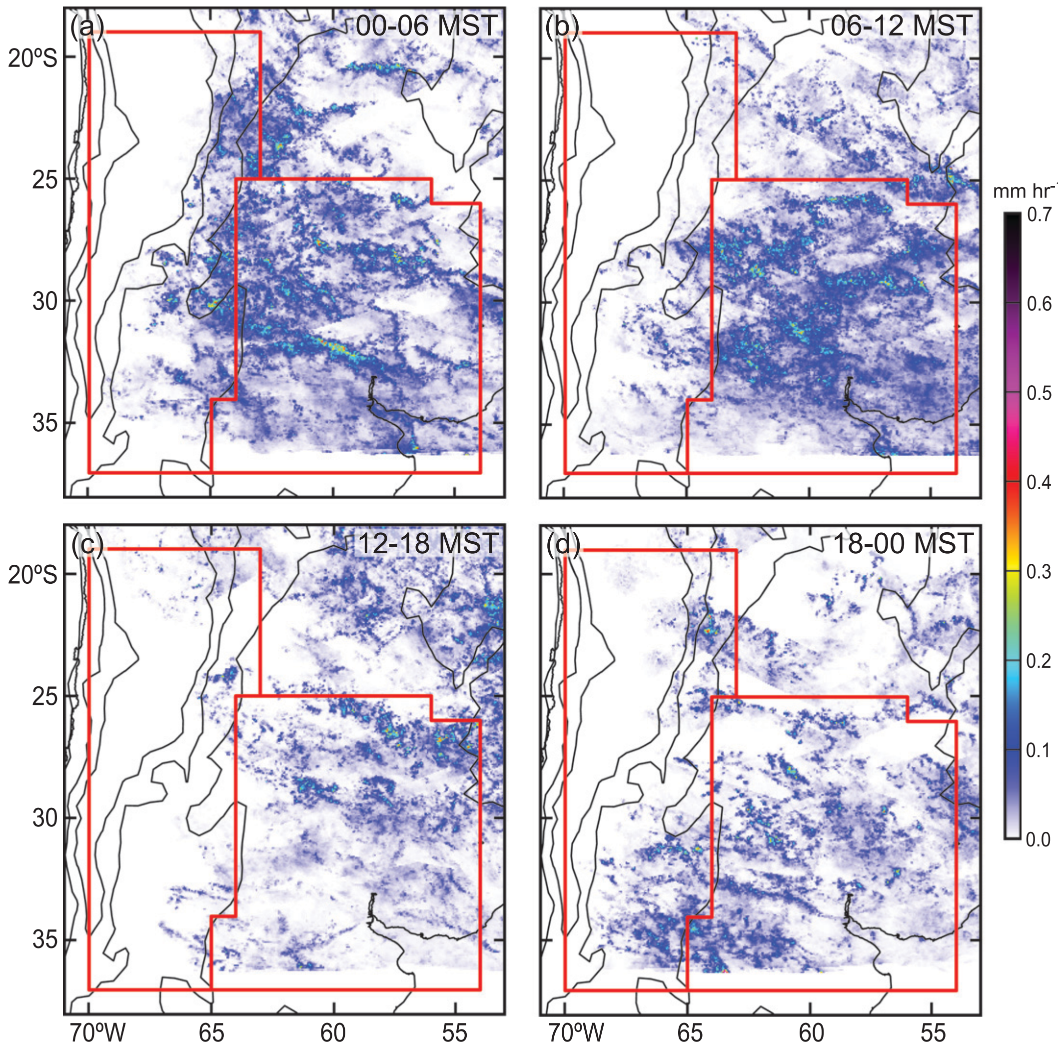

FIG. 9. As in Fig. 7 but for large echoes.

during the late night and early morning, which is especially pronounced for the strong large echo objects (Fig. 10f). The two-peak structure of the diurnal cycle is consistent with previous studies showing that the time of day of the peak precipitation varies on relatively small scales (Negri et al. 2000, 2002). The regional distribution of the precipitation from medium and large radar echoes is somewhat patchy. However, the afternoon precipitation is equally distributed over the whole region along with a band in the northeast with little precipitation (Figs. 12c and 13c). During the night and morning the prevailing strong systems have a tendency to occur in a region around 65°W, 7°S (Figs. 12a and 13a,b)—a region where previous analysis of just those systems containing extremely large stratiform regions has also shown a nocturnal maximum (Romatschke and Houze 2010). This nocturnal maximum also agrees with nocturnal precipitation peaks in the nearby cities of Humaitá and São Gabriel da Cachoeira (Angelis et al. 2004). This region also coincides with the region of maximum overall summertime precipitation in South America (Fig. 2a) and has been associated with the strengthening of Amazon squall lines, moving in from the northeast (Garstang et al. 1994), by large-scale convergence of water vapor flux (Labraga et al. 2000) and winds and increased moisture provided by the underlying rivers (Romatschke and Houze 2010). These squall lines form in the afternoon at the northeast coast near the mouths of the Amazon River and the Rio Tocantins (Garstang et al. 1994) where a maximum of precipitation from small, medium, and large convective systems occurs during that time of the day (northeast corner of the domain shown in Figs. 11c, 12c, and 13c).

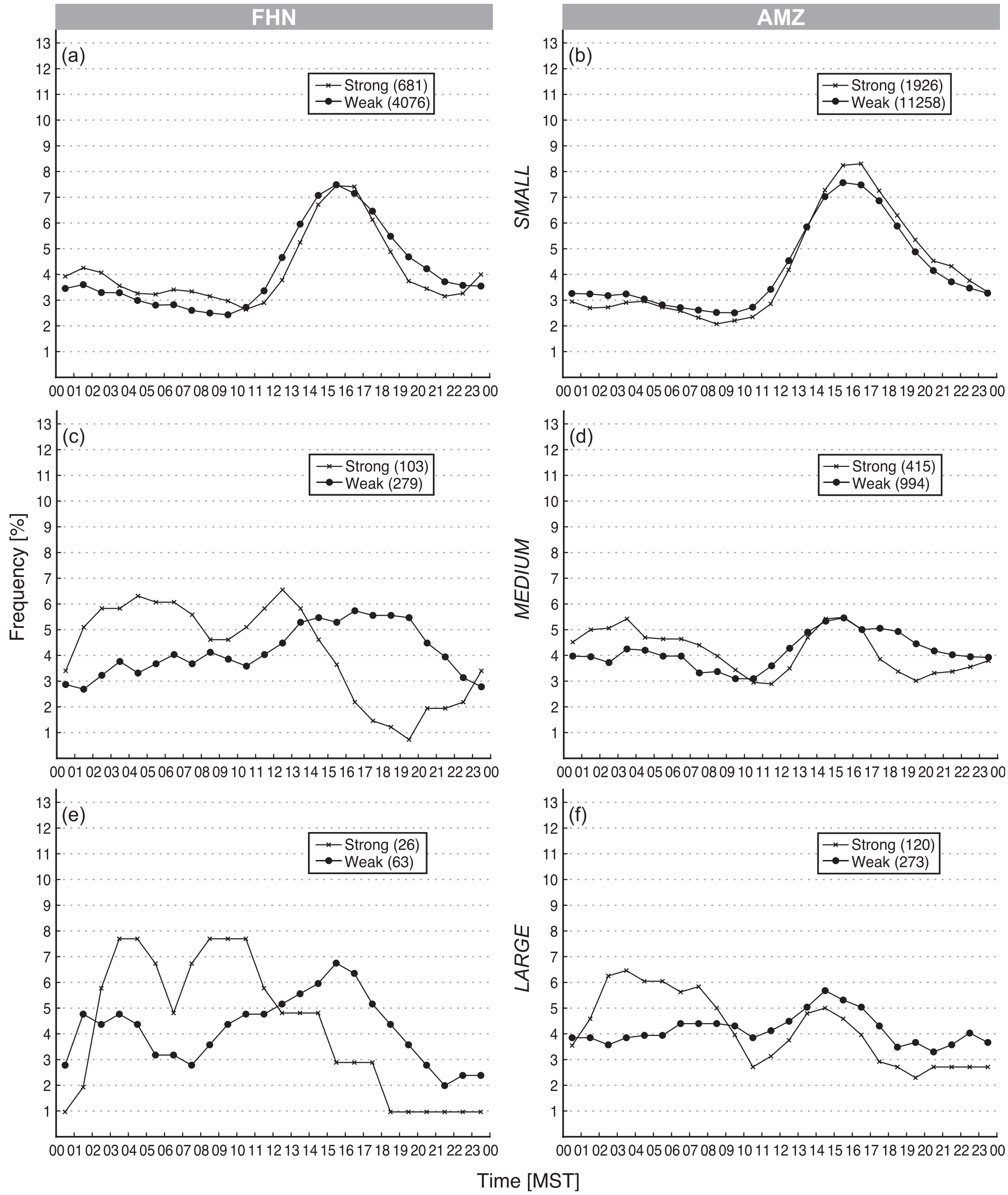

FIG. 10. As in Fig. 6 but for echoes in the FHN and AMZ regions.

c. South Atlantic convergence zone

Precipitation in the BHL region is mostly accounted for by small and medium radar echoes (Table 1, section 4b). However, the diurnal cycles of all radar echo types peak in the afternoon in the BHL region (Figs. 14a,c,e). Only the strong large echoes show a second peak during the late night, and it is very weak (Fig. 14e). Interestingly, in this region the strong echo objects show stronger peaks than the weak echoes, which indicates that the diurnal cycle of solar radiation in this region not only influences weaker daytime convection but also plays a significant role in the development of convective systems producing a lot of rain, which in other regions are often driven by other factors such as synoptic or orographic forcing, as has been discussed earlier.

The important rain-producing small and medium convective echoes are triggered in the afternoon over elevated terrain of the BHL region (cf. Fig. 1 with Figs. 15c and 16c). Romatschke and Houze (2010) found

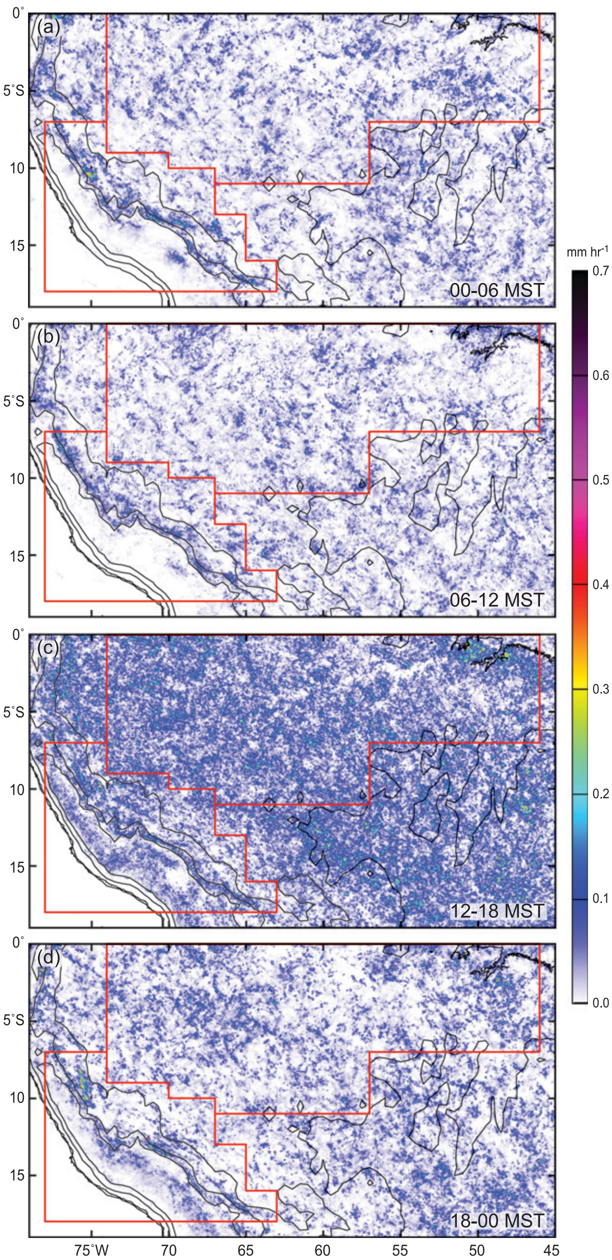

FIG. 11. As in Fig. 7 but for the continental tropics.

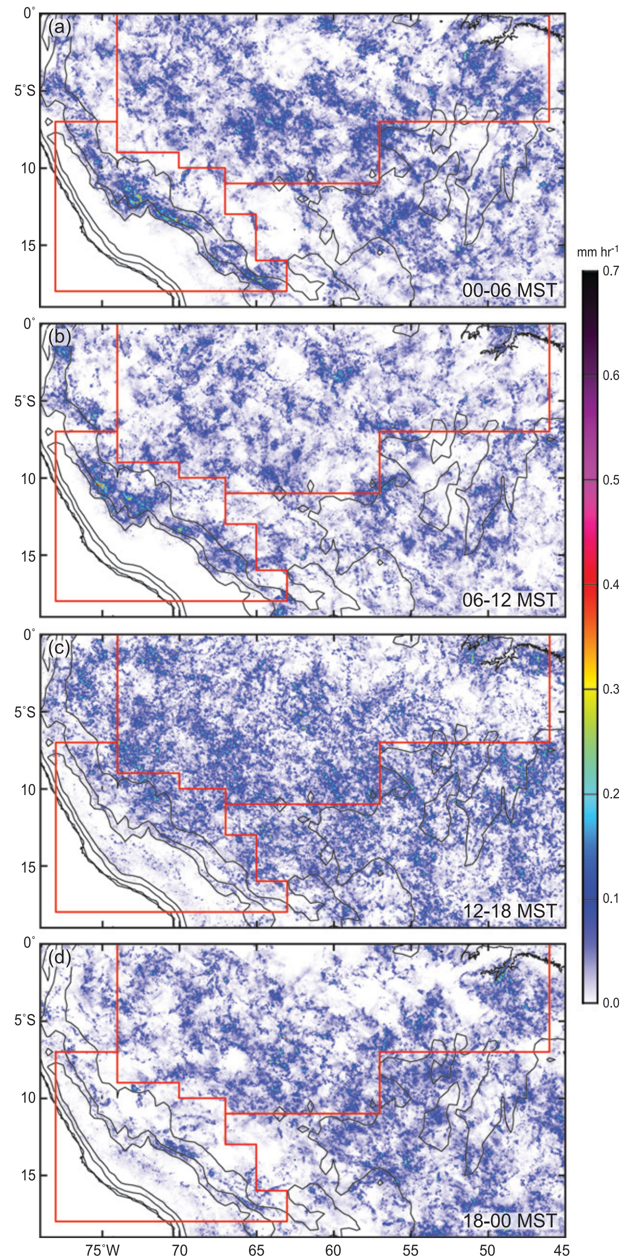

FIG. 12. As in Fig. 7 but for medium systems in the continental tropics.

that radar echoes containing extremely deep convective cores are triggered in the afternoon as moist flow from the ocean is lifted over the coastal mountains providing the additional lift that is needed to break through a cap of dry westerlies aloft. This capping mechanism is similar to the one in the FHS region (section 5a) and likely plays a role in the initiation of convection, especially along the coast.

Precipitation associated with the large echo objects in the BHL region, which form the peak in the afternoon, occurs primarily in the lowlands (cf. Figs. 1 and 17c). Precipitation in the northern part of the region is therefore associated with convection over the Amazon basin, whereas the echoes forming the stronger precipitation maximum in the south likely represent the latest stage of the convective systems associated with midlatitude trough passages. The convective systems that produce the late night peak are mostly located in the northern river valleys and may therefore be the result of local convergence of katabatic winds.

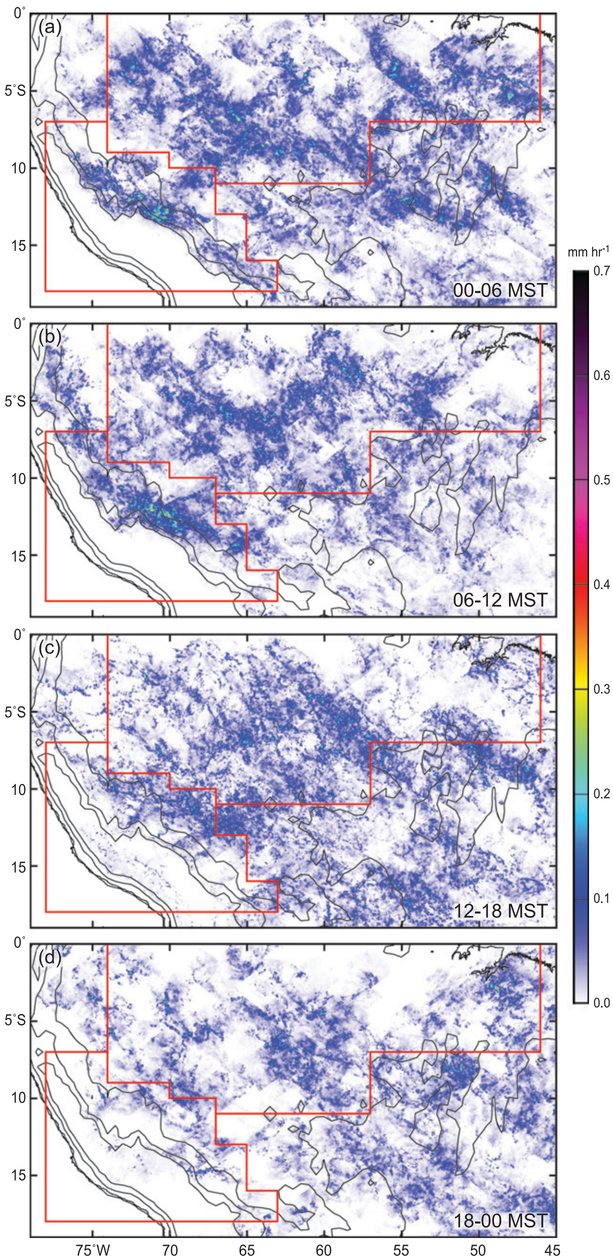

FIG. 13. As in Fig. 7 but for large systems in the continental tropics.

In the ATL region, most of the precipitation comes from the medium and especially the large echo object categories (Table 1). The diurnal cycles of the weak radar echoes of these categories have little amplitude (Figs. 14d,f). In contrast, the diurnal cycles for the strong echoes show both a broad maximum during the day and a minimum in the evening. The peak and minimum of the strong large echoes follow the peak and minimum of the strong medium echoes in time. Romatschke and Houze (2010) noted very similar diurnal cycles for convective systems containing wide areas of intense convective echo, which are followed by systems containing wide areas of stratiform echo. They suggested that the evening minimum in extreme convective systems is a result of weakened convergence in this region as a result of air being drawn inland as a late response to the diurnal heating and convergence over the continent. The fact that strong medium echoes, which apparently contain wide areas of strong convection, are followed in time by large echoes with wide areas of stratiform echo indicates that they likely represent early and late stages of convective system development, respectively. Similar mechanisms leading to similar daily cycles of convective systems have also been observed over the Bay of Bengal in the South Asian premonsoon and monsoon (Romatschke and Houze 2011a,b).

6. Conclusions

Ten years of TRMM data have been used to investigate the precipitation patterns of South America in relation to the types of radar echoes associated with the rainfall. We have categorized the rainfall according to the characteristics of the radar echoes with which the rain was associated to gain an understanding of the physical mechanisms associated with the most important rain-producing convective systems. These investigations are possible because the TRMM PR provides information on both the detailed patterns of rain accumulations and on the radar-echo structures of the storms producing the rainfall.

The ability of the precipitation radar to determine three-dimensional echo structure as well as echo intensity has allowed us to categorize precipitating cloud systems into those comprising small, medium, and large contiguous radar-echo objects. These size categories are defined such that each category explains 30% of the total precipitation. The many tiny echoes accounting for the remaining 10% are ignored. Within each of the 30% categories, the radar echoes are further subdivided into subcategories of ''strong'' and ''weak'' systems, where the strong ones are those echo objects that are bigger than the median dividing their combined rainfall amount in half. The weak and strong echoes of the 30% size categories were further examined to determine their convective nature in terms of three convection variables: maximum height and area fraction of convective echoes exceeding 40-dBZ reflectivity values and convective rain fraction. Of the variables investigated, the overall echo object size is found to be the property most strongly related to the precipitation production of convective systems. The three convection variables were

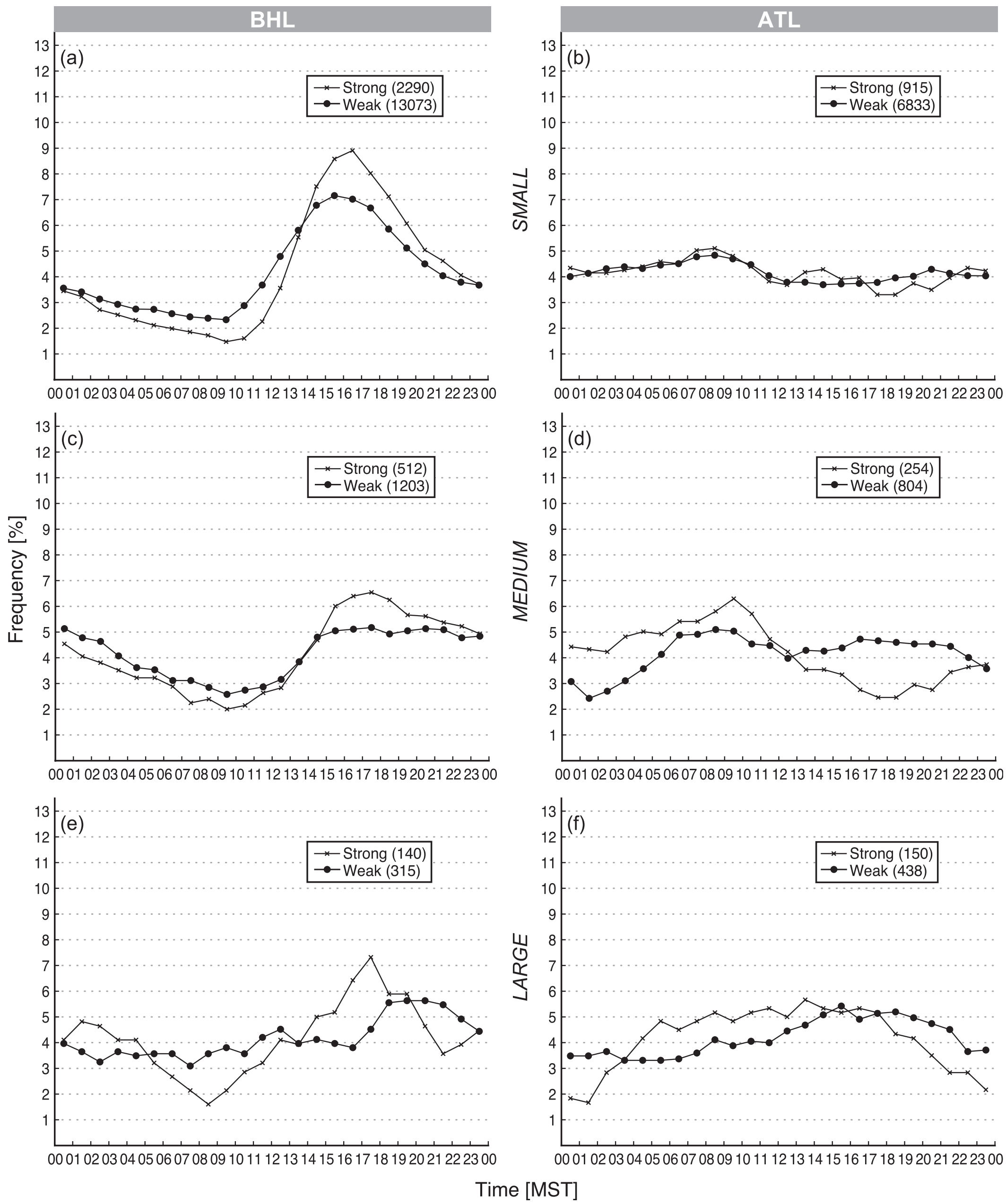

FIG. 14. As in Fig. 6 but for systems in the BHL and ATL regions.

related only slightly to precipitation production, especially for smaller convective systems. These overall convection variables may, however, not give a complete picture of the role of convection in the rainfall of South America. We have yet to separate especially high-impact convective events to assess their particular role in precipitation production. Further research is under way to determine whether extreme convective events [as defined, for example, in the previous studies of Houze et al. (2007), Romatschke et al. (2010), and Romatschke and Houze (2010)] are related to rainfall production more strongly than these overall convective properties.

In the continental subtropics, at the southern foothills of the Central Andes, most of the precipitation comes from systems of small horizontal dimension but featuring extremely deep convective cells, which are first triggered in the afternoon. Over the La Plata basin, large echo objects account for the largest portion of precipitation. These large echo objects occur in early to midmorning, consistent with the convective cells generated

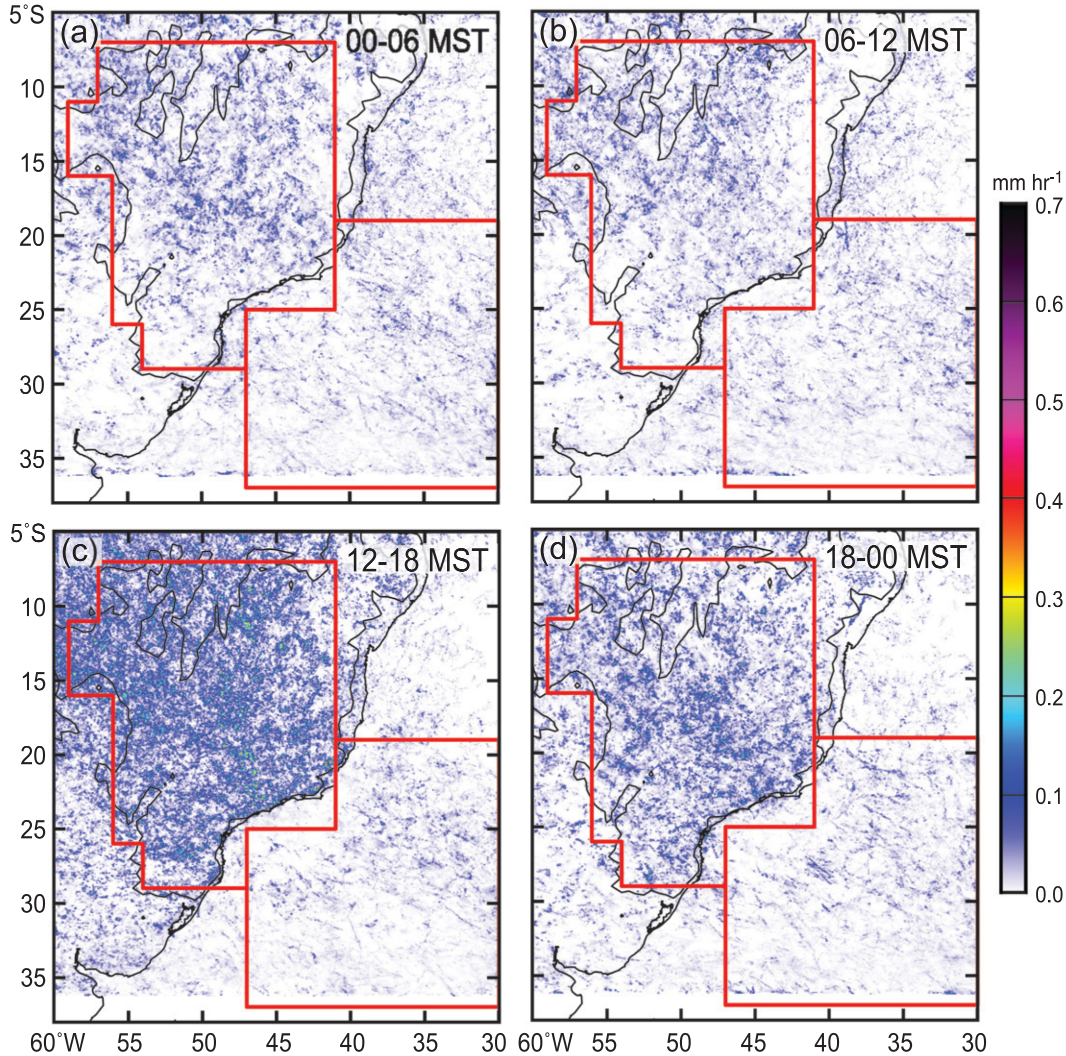

FIG. 15. As in Fig. 7 but for small systems in the SACZ.

diurnally over the lower foothills of the Andes growing into eastward-moving mesoscale convective systems of the type that have been described previously (Nicolini and Saulo 2006; Saulo et al. 2007; Matsudo and Salio 2011; Rasmussen and Houze 2011). These systems are evidently maintained by generation of new convection at a front and/or mesoscale cold pool boundaries and maximize at a later time of day owing to their eastward movement and the input of low-level moisture from the nocturnally modulated SALLJ.

In the continental tropics precipitation is produced from convective systems with radar echoes in all three size categories with slightly larger amounts coming from systems in smaller categories. In general, continental tropical precipitating cloud systems are more stratiform in nature than in the subtropics. Small radar echoes, weak medium echoes, and weak large echoes peak in the afternoon, probably as a result of increased solar heating. Strong medium and large echoes show a nighttime-to-morning peak in their diurnal cycle. Over the Amazon basin they have an additional afternoon peak. The nocturnal systems are major rain producers and feature large regions of extreme convection in early stages of their life cycle and large regions of stratiform rain at later stages (Romatschke and Houze 2010). At the northern foothills of the Central Andes a nocturnal precipitation maximum is associated with large and medium radar echoes. In this region, these major rain-producing convective systems likely form as the moist low-level flow from the Amazon basin is lifted over the foothills and possibly converges with nocturnal downslope flow from the Andes. During

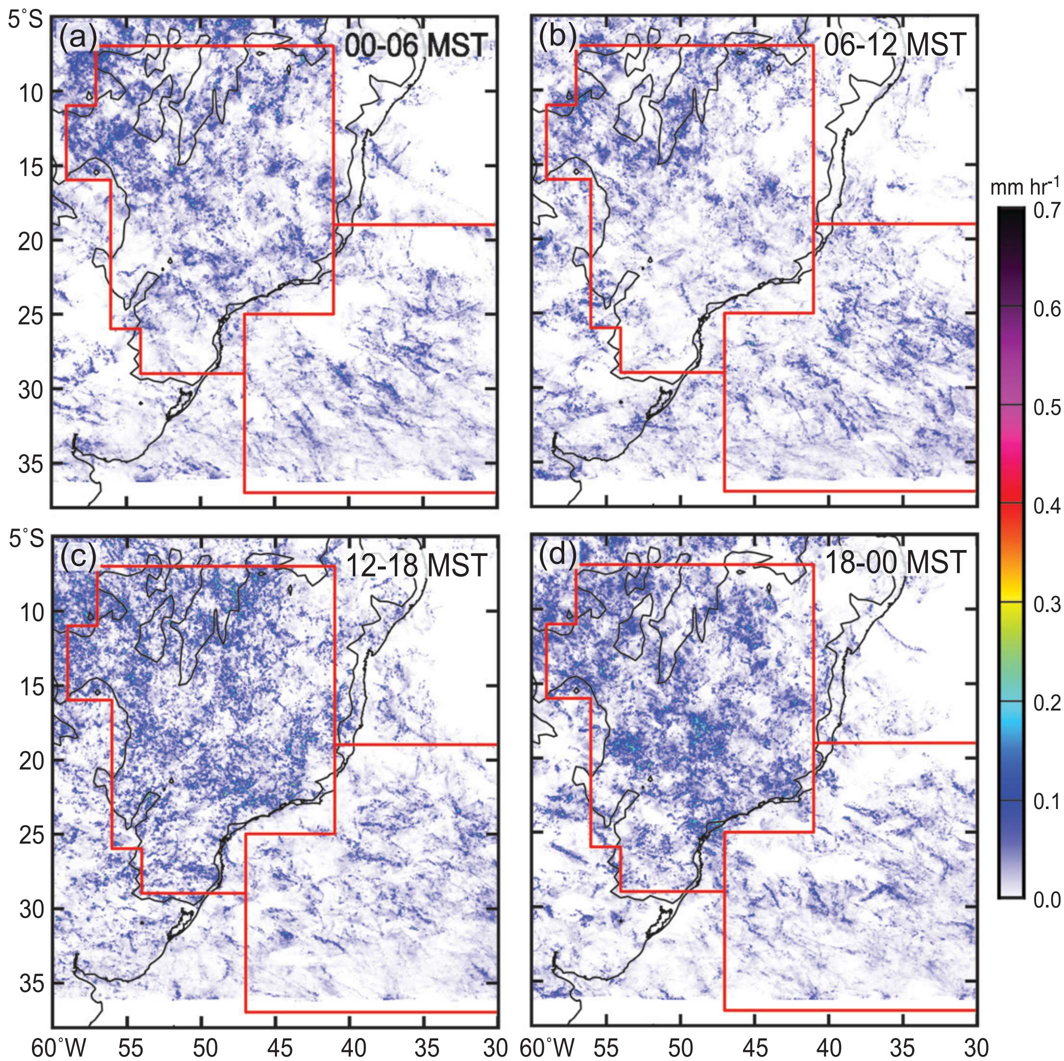

FIG. 16. As in Fig. 7 but for medium systems in the SACZ.

the day this process is counteracted by divergence at the foothills, which is associated with convergence over the mountains and resulting upslope flow. Over the Amazon basin, diurnal precipitation dominates; however, in some regions nocturnal precipitation maxima are observed, which are likely associated with the medium and large nocturnal radar echoes mentioned above. Because of the intermittent sampling of TRMM, the likely important role of the squall lines that are known to be triggered at the northeast coast during the afternoon and move over the Amazon basin in a northeast to southwest direction remains unclear, as does the amount of precipitation they account for.

Over the Brazilian Highlands, precipitation from small convective clouds occurs first in the afternoon over higher terrain. Most of the precipitation is associated with these small echoes, which are very convective in nature and are known to feature extremely deep convective cores. They grow to medium and even large size in the evening. All types of echoes in this region show afternoon or evening peaks in their diurnal cycle. Only strong large echoes show an additional peak during the late night, which is apparently associated with precipitation maxima in local river valleys. The afternoon and evening peaks in the diurnal cycles underscore the important role of solar heating for the precipitation in this region. The larger echoes in this region are likely also controlled by the tendency of this region to be occupied by a synoptic-scale low pressure system (Romatschke and Houze 2010).

Over the eastern South Atlantic in the SACZ most of the precipitation is associated with medium and very

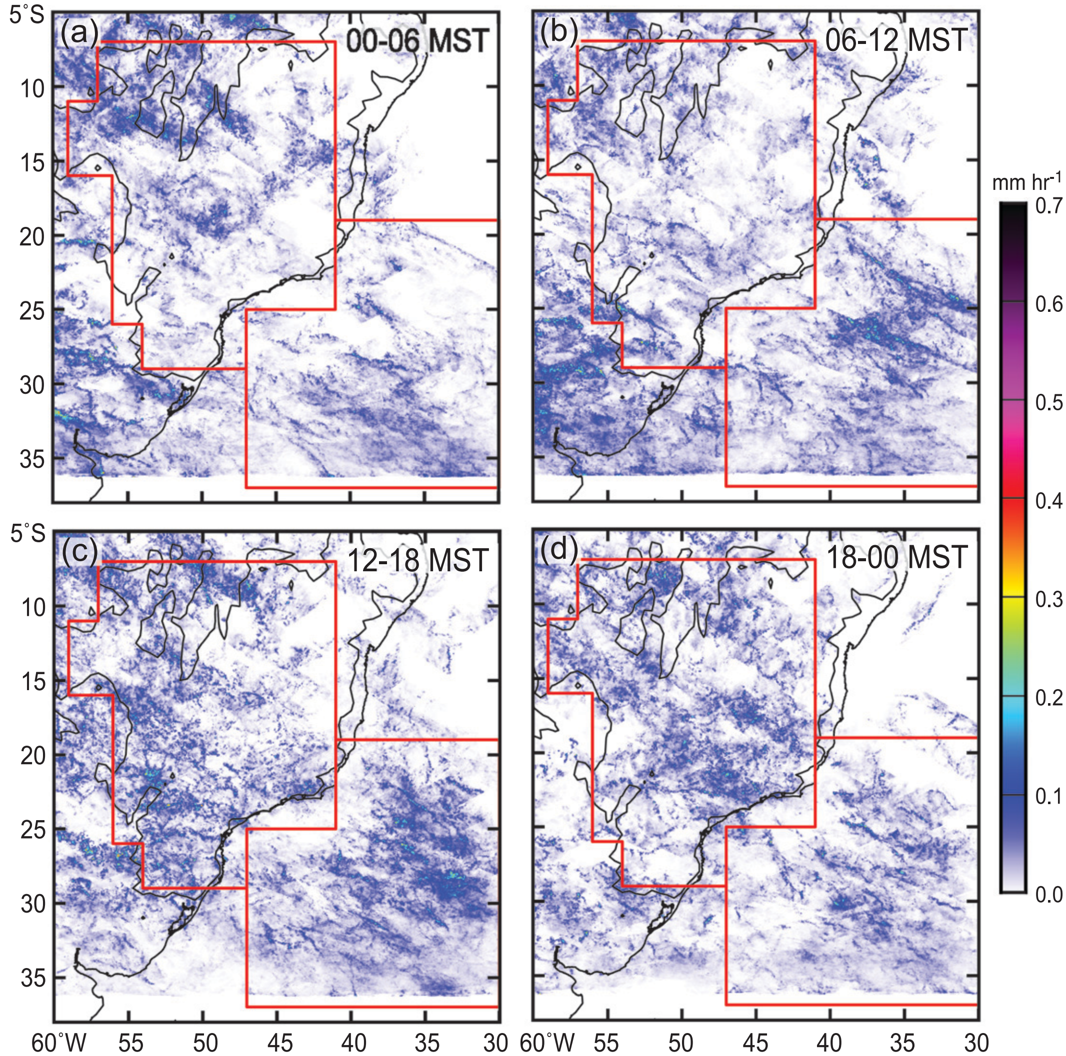

FIG. 17. As in Fig. 7 but for large systems in the SACZ.

large echoes. They develop in an environment of an anomalous synoptic low at the same location. The diurnal cycles of medium and large echoes show minima during the evening and early night, respectively, and broad maxima during the day. Medium echoes, which may contain large areas of extreme convection, have earlier maxima and minima than large echoes, which may contain wide areas of stratiform rain—which indicates that they represent the same systems at earlier and later stages of their life cycle, respectively. The minima during the evening are likely a late response to the diurnal heating over the continent that draws air inland and thereby weakens the convergence in the SACZ.

When combining the results of this study with the results of Romatschke and Houze (2010) it is interesting to note that the physical mechanisms leading to the development of strongly precipitating systems, that is, the strong system categories, studied here, are basically the same as those leading to the development of extreme forms of convection studied by Romatschke and Houze (2010). This finding is not surprising since one would expect extreme types of systems to produce a lot of rain. However, by including all precipitation-producing systems the current study not only qualitatively but quantitatively identifies the types of systems that need attention from a hydrologic point of view.

Acknowledgments. We acknowledge Carol Archambeault of NASA for providing the TRMM PR data. The NCEP CFSR data are from the Research Data Archive (RDA), which is maintained by the Computational and Information Systems Laboratory (CISL) at the National Center for Atmospheric Research (NCAR). NCAR is sponsored by the National Science Foundation (NSF). The original data are available from the RDA (http://rda.ucar.edu) in dataset number ds093.0. Beth Tully edited the manuscript and designed the graphics. This research was supported by the National Science Foundation under Grants ATM-0505739, AGS-0820586, AGS-1144105, and by the National Aeronautics and Space Administration under Grants NNX07AD59G and NNX10AH70G.

REFERENCES

Altinger de Schwarzkopf, M. L., and L. C. Rosso, 1982: Severe storms and tornadoes in Argentina. Preprints, *12th Conf. on Severe Local Storms,* San Antonio, TX, Amer. Meteor. Soc., 59–62.

Anabor, V., D. J. Stensrud, and O. L. L. de Moraes, 2008: Serial upstream-propagating mesoscale convective system events over southeastern South America. *Mon. Wea. Rev.,* **136,** 3087–3105.

——, ——, and ——, 2009: Simulation of a serial upstream-propagating mesoscale convective system event over southeastern South America using composite initial conditions. *Mon. Wea. Rev.,* **137,** 2144–2163.

Angelis, C. F., G. R. McGregor, and C. Kidd, 2004: Diurnal cycle of rainfall over the Brazilian Amazon. *Climate Res.,* **26,** 139–149.

Awaka, J., T. Iguchi, H. Kumagai, and K. Okamoto, 1997: Rain type classification algorithm for TRMM Precipitation Radar. *Proc. IGARSS '97,* Singapore, IEEE International, 1633–1635.

Carvalho, L. M. V., C. Jones, and M. A. F. Silva Dias, 2002: Intraseasonal large-scale circulations and mesoscale convective activity in tropical South America during the TRMM-LBA campaign. *J. Geophys. Res.,* **107,** 8042, doi:10.1029/2001JD000745.

De Angelis, C. F., G. R. Mcgregor, and C. Kidd, 2004: A 3 year climatology of rainfall characteristics over tropical and subtropical South America based on tropical rainfall measuring mission precipitation radar data. *Int. J. Climatol.,* **24,** 385–399.

Durkee, J. D., T. L. Mote, and J. M. Shepherd, 2009: The contribution of mesoscale convective complexes to rainfall across subtropical South America. *J. Climate,* **22,** 4590–4605.

Garreaud, R. D., and J. M. Wallace, 1997: The diurnal march of convective cloudiness over the Americas. *Mon. Wea. Rev.,* **125,** 3157–3171.

——, and ——, 1998: Summertime incursions of midlatitude air into subtropical and tropical South America. *Mon. Wea. Rev.,* **126,** 2713–2733.

Garstang, M., H. L. Massie, J. Halverson, S. Greco, and J. Scala, 1994: Amazon coastal squall lines. Part I: Structure and kinematics. *Mon. Wea. Rev.,* **122,** 608–622.

Giovannettone, J. P., and A. P. Barros, 2009: Probing regional orographic controls of precipitation and cloudiness in the central Andes using satellite data. *J. Hydrometeor.,* **10,** 167–182.

Halverson, J. B., T. Rickenbach, B. Roy, H. Pierce, and E. Williams, 2002: Environmental characteristics of convective systems during TRMM-LBA. *Mon. Wea. Rev.,* **130,** 1493–1509.

Houze, R. A., Jr., 2004: Mesoscale convective systems. *Rev. Geophys.,* **42,** RG4003, doi:10.1029/2004RG000150.

——, D. C. Wilton, and B. F. Smull, 2007: Monsoon convection in the Himalayan region as seen by the TRMM Precipitation Radar. *Quart. J. Roy. Meteor. Soc.,* **133,** 1389–1411.

Iguchi, T., R. Meneghini, J. Awaka, T. Kozu, and K. Okamoto, 2000: Rain profiling algorithm for TRMM Precipitation Radar data. *Adv. Space Res.,* **25,** 973–976.

Kikuchi, K., and B. Wang, 2008: Diurnal precipitation regimes in the global tropics. *J. Climate,* **21,** 2680–2696.

Kummerow, C., W. Barnes, T. Kozu, J. Shiue, and J. Simpson, 1998: The Tropical Rainfall Measuring Mission (TRMM) sensor package. *J. Atmos. Oceanic Technol.,* **15,** 809–817.

——, and Coauthors, 2000: The status of the Tropical Rainfall Measuring Mission (TRMM) after two years in orbit. *J. Appl. Meteor.,* **39,** 1965–1982.

Labraga, J. C., O. Frumento, and M. López, 2000: The atmospheric water vapor cycle in South America and the tropospheric circulation. *J. Climate,* **13,** 1899–1915.

Laurent, H., L. A. T. Machado, C. A. Morales, and L. Durieux, 2002: Characteristics of the Amazonian mesoscale convective systems observed from satellite and radar during the WETAMC/LBA experiment. *J. Geophys. Res.,* **107,** 8054, doi:10.1029/2001JD000337.

Lenters, J. D., and K. H. Cook, 1995: Simulation and diagnosis of the regional summertime precipitation climatology of South America. *J. Climate,* **8,** 2988–3005.

——, and ——, 1999: Summertime precipitation variability over South America: Role of the large-scale circulation. *Mon. Wea. Rev.,* **127,** 409–431.

Liebmann, B., G. N. Kiladis, J. A. Marengo, T. Ambrizzi, and J. D. Glick, 1999: Submonthly convective variability over South America and the South Atlantic convergence zone. *J. Climate,* **12,** 1877–1891.

——, ——, C. S. Vera, A. C. Saulo, and L. M. V. Carvalho, 2004: Subseasonal variations of rainfall in South America in the vicinity of the low-level jet east of the Andes and comparison to those in the South Atlantic convergence zone. *J. Climate,* **17,** 3829–3842.

Machado, L. A. T., W. B. Rossow, R. L. Guedes, and A. W. Walker, 1998: Life cycle variations of mesoscale convective systems over the Americas. *Mon. Wea. Rev.,* **126,** 1630–1654.

Maddox, R. A., 1980: Mesoscale convective complexes. *Bull. Amer. Meteor. Soc.,* **61,** 1374–1387.

Marengo, J. A., W. R. Soares, C. Saulo, and M. Nicolini, 2004: Climatology of the low-level jet east of the Andes as derived from the NCEP–NCAR reanalyses: Characteristics and temporal variability. *J. Climate,* **17,** 2261–2280.

Matsudo, C. M., and P. V. Salio, 2011: Severe weather reports and proximity to deep convection over Northern Argentina. *Atmos. Res.,* **100,** 523–537.

Meneghini, R., J. A. Jones, T. Iguchi, K. Okamoto, and J. Kwiatkowski, 2001: Statistical methods of estimating average rainfall over large space–timescales using data from the TRMM precipitation radar. *J. Appl. Meteor.,* **40,** 568–585.

Mezher, R. N., M. Doyle, and V. Barros, 2012: Climatology of hail in Argentina. *Atmos. Res.,* **114–115,** 70–82.

Negri, A. J., E. N. Anagnostou, and R. F. Adler, 2000: A 10-yr climatology of Amazonian rainfall derived from passive microwave satellite observations. *J. Appl. Meteor.,* **39,** 42–56.

——, L. Xu, and R. F. Adler, 2002: A TRMM-calibrated infrared rainfall algorithm applied over Brazil. *J. Geophys. Res.,* **107,** 8048, doi:10.1029/2000JD000265.

Nesbitt, S. W., and E. J. Zipser, 2003: The diurnal cycle of rainfall and convective intensity according to three years of TRMM measurements. *J. Climate,* **16,** 1456–1475.

Nicolini, M., and A. C. Saulo, 2006: Modeled Chaco low-level jets and related precipitation patterns during the 1997–1998 warm season. *Meteor. Atmos. Phys.,* **94,** 129–143.

Nieto Ferreira, R., T. M. Rickenbach, D. L. Herdies, and L. M. V. Carvalho, 2003: Variability of South American convective cloud systems and tropospheric circulation during January–March 1998 and 1999. *Mon. Wea. Rev.,* **131,** 961–973.

Nogués-Paegle, J., and K. C. Mo, 1997: Alternating wet and dry conditions over South America during summer. *Mon. Wea. Rev.,* **125,** 279–291.

Pereira, L. G., and S. A. Rutledge, 2006: Diurnal cycle of shallow and deep convection for a tropical land and an ocean environment and its relationship to synoptic wind regimes. *Mon. Wea. Rev.,* **134,** 2688–2701.

Petersen, W. A., S. W. Nesbitt, R. J. Blakeslee, R. Cifelli, P. Hein, and S. A. Rutledge, 2002: TRMM observations of intraseasonal variability in convective regimes over the Amazon. *J. Climate,* **15,** 1278–1294.

Rasmussen, K. L., and R. A. Houze Jr., 2011: Orogenic convection in South America as seen by the TRMM satellite. *Mon. Wea. Rev.,* **139,** 2399–2420.

Rickenbach, T. M., R. Nieto Ferreira, J. B. Halverson, D. L. Herdies, and M. A. F. Silva Dias, 2002: Modulation of convection in the southwestern Amazon basin by extratropical stationary fronts. *J. Geophys. Res.,* **107,** 8040, doi:10.1029/2000JD000263.

Romatschke, U., and R. A. Houze Jr., 2010: Extreme summer convection in South America. *J. Climate,* **23,** 3761–3791.

——, and ——, 2011a: Characteristics of precipitating convective systems in the South Asian monsoon. *J. Hydrometeor,* **12,** 3–26.

——, and ——, 2011b: Characteristics of precipitating convective systems in the premonsoon season of South Asia. *J. Hydrometeor,* **12,** 157–180.

——, S. Medina, and R. A. Houze Jr., 2010: Regional, seasonal, and diurnal variations of extreme convection in the South Asian region. *J. Climate,* **23,** 419–439.

Salio, P., M. Nicolini, and E. J. Zipser, 2007: Mesoscale convective systems over southeastern South America and their relationship with the South American low-level jet. *Mon. Wea. Rev.,* **135,** 1290–1309.

Saulo, C., J. Ruiz, and Y. G. Skabar, 2007: Synergism between the low-level jet and organized convection at its exit region. *Mon. Wea. Rev.,* **135,** 1310–1326.

Silva Dias, M. A. F., 2011: An increase in the number of tornado reports in Brazil. *Wea. Climate Soc.,* **3,** 209–217.

Siqueira, J. R., and L. A. T. Machado, 2004: Influence of the frontal systems on the day-to-day convection variability over South America. *J. Climate,* **17,** 1754–1766.

——, W. B. Rossow, L. A. T. Machado, and C. Pearl, 2005: Structural characteristics of convective systems over South America related to cold-frontal incursions. *Mon. Wea. Rev.,* **133,** 1045–1064.

Velasco, I., and J. M. Fritsch, 1987: Mesoscale convective complexes in the Americas. *J. Geophys. Res.,* **92** (D8), 9591–9613.

Zamboni, L., C. R. Mechoso, and F. Kucharski, 2010: Relationships between upper-level circulation over South America and rainfall over southeastern South America: A physical base for seasonal predictions. *J. Climate,* **23,** 3300–3315.

Zipser, E. J., D. J. Cecil, C. Liu, S. W. Nesbitt, and D. P. Yorty, 2006: Where are the most intense thunderstorms on Earth? *Bull. Amer. Meteor. Soc.,* **87,** 1057–1071.